Chapter 3
Extreme-impedance measurements

3.1 The impedance matching challenge in RF nanoelectronics

Microwave measurements of RF nanoelectronic devices present numerous challenges. Among these, perhaps the most difficult measurement challenge arises from the inherent, often extreme impedance mismatch between nanolectronic systems and conventional commercial test equipment. The physical origin of this mismatch may be understood by comparing two physical constants: the free space impedance and the quantum resistance [1]. The impedance of free space Z_{free} is given by the ratio of the magnitude of the electric field component to the magnitude of the magnetic field component in a TEM (or far field) electromagnetic wave:

$$Z_{free} = \frac{E}{H} = \sqrt{\frac{\mu_0}{\varepsilon_0}} = 377\ \Omega\ , \tag{3.1}$$

where μ_0 is the permeability of free space, ε_0 is the permittivity of free space, and E and H are the magnitudes of the electric and magnetic field components, respectively. Recall from Section 2.2 that the impedance of the TE mode in a waveguide is given by the product of Z_{free} times a ratio of the wavelengths of a given mode in free space and in a waveguide and that the impedance of the TM mode is given by Z_{free} divided by this same ratio. Thus, the value of Z_{free} sets the natural impedance range for both free space and guided waves. As a result, the relevant commercial test equipment has been developed to match this impedance scale. By contrast, the quantum resistance is given by:

$$R_Q = \frac{h}{2e^2} = 12.9\ k\Omega \tag{3.2}$$

where h is Planck's constant and e is the charge of an electron. Experimentally, the conductance of a two-dimensional electron gas, such as those found in high electron mobility transistors or single-layer graphene, takes on quantized values proportional to $1/R_Q$ [2]. This effect is known as the quantum Hall effect and occurs only at cryogenic temperatures and in the presence of a high magnetic field. More broadly, the resistance of nano-electronic devices with dimensions of the order of the de Broglie wavelength of an electron is on the order of the quantum resistance. In the particular case of a single-walled carbon nanotube, the resistance is $R_Q/2$ [1] (the factor of two arises from band structure degeneracy).

The vastly different scales of Z_{free} and R_Q illustrate the inherent impedance mismatch between the nanoelectronic world and conventional microwave measurements. As a consequence of impedance mismatch, directly connecting a calibrated network analyzer to an extreme impedance device will not usually yield meaningful measurements. Most of the signal incident on the extreme impedance device will be reflected back to the analyzer. Alternative approaches to extreme impedance measurements must be developed. Before discussing specific applications of such approaches to RF nanoelectronics in Chapter 4, we will discuss extreme-impedance measurements more generally in the remainder of this

chapter. Because the impedance of nanoelectronic devices is generally much greater than that of commercial test equipment, the methods we discuss have primarily been developed and verified for extremely high impedance measurements. The methods should be applicable to extremely low impedance measurements, but to date extension of these methods to extremely low impedances has been limited.

3.2 An introduction to extreme-impedance measurements

Consider a one-port, microwave network terminated by a load impedance of $Z_L = \alpha_L + \beta_L j$. The complex reflection coefficient from the load, Γ_L, is given by

$$\Gamma_L = \frac{Z_L - Z_0}{Z_L + Z_0}, \tag{3.3}$$

where Z_0 is the characteristic impedance of the guided-wave network that is connected to the load. For most guided-wave networks, including coaxial- and waveguide-based transmission, the characteristic impedance is typically $Z_0 = 50\ \Omega$ (or in a few cases 75 Ω). For free space measurements, the characteristic impedance is 377 Ω. Equation (3.3) is plotted in Fig. 3.1(a) for the case $Z_L = \alpha_L$, with $\beta_L = 0$. In order to maximize the signal transmitted to the load, impedances of microwave devices are designed to match the characteristic impedance. In general, the matching condition is that the load impedance should be equal to the characteristic impedance:

$$Z_L = Z_0 \ . \tag{3.4}$$

Note that this condition differs from the condition for maximum power transfer to the load, which occurs when the load impedance is equal to the complex conjugate of the characteristic impedance. Historically, approaches to calibration and measurement of microwave devices have been developed, tested, and optimized for devices-under-test that are reasonably well-matched, meeting or nearly meeting the condition in Equation (3.4). By contrast, if the load impedance is much larger or much smaller than the characteristic impedance, the magnitude of Γ_L will approach one. In such cases, most of the incident microwave signal will be reflected from the device and little if any signal will be transmitted to the load.

Figure 3.1. **Reflection coefficient Γ_L for a one-port network.** (a) The one-port reflection coefficient Γ_L of a one port network connected to a load impedance Z_L as a function of normalized impedance Z_L/Z_0 for the case $Z_L = \alpha_L$ ($b_L = 0$). (b) The derivative of Γ_L with respect to the normalized impedance Z_L/Z_0 for the case $Z_L = \alpha_L$ ($b_L = 0$). The vertical dashed line corresponds to a matched impedance ($Z_L = Z_0$) in both (a) and (b).

For many RF nanoelectronic devices, the device under test does indeed possess an extreme impedance that is far from the reference impedance, giving rise to new measurement challenges. First, the measured values of Γ_L will differ only slightly from one. As a specific example, for a resistive device with impedance on the order of one resistance quantum (Z_L = 12.9 kΩ), $|\Gamma_L| = 0.9923$. Over ninety-nine percent of the incident power is reflected from the device! In other words, $|\Gamma_L|$ will differ from an open circuit, for which $|\Gamma_L|$ is unity, by

only a few parts in one thousand. Furthermore, measurements of Γ_L for high impedance devices are insensitive to changes in Z_L. Taking the derivative of Equation (3.3) with respect to the normalized impedance Z_L/Z_0 yields:

$$\frac{\delta\Gamma_L}{\delta(\frac{Z_L}{Z_0})} = \frac{2Z_0}{(Z_L+Z_0)^2} \ . \tag{3.5}$$

Equation (3.5) is plotted in Fig. 3.1(b) for the case $Z_L = \alpha_L$ with $\beta_L = 0$. Note that $d\Gamma_L/d(Z_L/Z_0)$ falls off as Z_L is increased from Z_0 to higher values, rapidly approaching zero. This indicates that a one-port measurement of Γ_L will be insensitive to changes in Z_L if Z_L is greater than or on the order of 10 Z_0, even if those changes are quite substantial.

One way to visualize the extreme impedance problem is through the Smith chart, as illustrated in Fig. 3.2. Recall from Chapter 2 that for a one port network, the center of the Smith chart corresponds to the point where the load is perfectly impedance-matched and the reflection coefficient is zero. By contrast, extreme-impedance measurements represented on a Smith chart will lie near the edge of the chart, as shown by the shaded region in Fig. 3.2. In the particular case of RF nanoelectronics measurements, the impedance will lie near the right hand edge of the chart, corresponding to extremely high impedance. In this region of the Smith chart, the magnitude of the reflection coefficient approaches one. In addition, there is a high density of constant resistance circles and constant reactance curves in this region of the Smith chart. This visually illustrates that substantial changes in extremely high Z_L will result in only a small translation on the Smith chart.

Figure 3.2. **Smith chart representation of the extreme impedance measurement problem.** Extreme impedance loads are represented by the shaded grey region near the circumference of the Smith chart, with most RF Nanoelectronics devices (*RF NANO*) falling near the right edge of the chart. Interferometry is one strategy for moving the measurand from the edge of the chart closer to the characteristic impedance Z_0.

In summary, the closeness of the one-port reflection coefficient Γ_L to unity and the relative insensitivity of Γ_L to changes in Z_L, present significant measurement challenges. Note that these challenges arise from the attempt to directly measure Γ_L. One alternative strategy is to re-configure the measurement platform in order to measure an alternate quantity that is better matched and more sensitive to Z_L. Graphically, this re-configuration can be envisioned as a translation from the edge of the Smith chart to the center, as shown by the black arrow in Fig. 3.2. Interferometry is one effective approach to moving the measurand from the edge to the center of the Smith chart. A drawback of this strategy is that additional calibration and analysis steps may be required to obtain the desired measurement from the alternate, well-matched measurand. Four specific approaches will be discussed here. The first is a simple impedance matching network, which may be useful particularly when the nanoelectronic device has a narrow operating bandwidth. The other three approaches are interferometric: a reflectometer based on a power splitter, a reflectometer based on a hybrid coupler, and an interferometer with active signal injection. Below, the discussion of these four approaches will be restricted to guided-wave structures, but the approaches can be generalized to an on-wafer environment.

3.3 Impedance matching networks

Perhaps the most common, traditional approach to impedance mismatch problems is the introduction of an impedance matching network. Consider the measurement of a device under test (DUT) with impedance Z_{DUT}, as shown in Fig. 3.3(a). An impedance matching network has been inserted between the test equipment and the DUT. In general, there are a wide range of possible circuit configurations for matching networks and a great deal of engineering has historically been devoted to the impedance matching problem. Here, we will consider only a simple case consisting of a series impedance Z_S and a parallel impedance Z_P, as shown in Fig. 3.3(b). This simple configuration is useful for cases where Z_{DUT} is much larger than Z_0, which is nearly always the case for RF nanoelectronic devices. With this matching network in place, the total load impedance is now

$$Z_L = Z_S + \frac{Z_P Z_{DUT}}{Z_P + Z_{DUT}} \quad . \tag{3.6}$$

In order for the inserted elements to function as an impedance matching network, the values of Z_S and Z_P are chosen so that Equation (3.4) is satisfied.

Figure 3.3 **Schematic of an impedance matching network.** (a) A matching network is inserted between the test equipment (reference impedance Z_0) and the device under test (impedance Z_{DUT}). (b) One example of an implementation of a matching network.

When the extreme impedance of the DUT is well known, the implementation of a fixed impedance matching network may be an effective tool for facilitating the measurement over a finite bandwidth. Combining Equations (3.4) and (3.6), we find

$$Z_0^* = Z_S + \frac{Z_P Z_{DUT}}{Z_P + Z_{DUT}} \quad . \tag{3.7}$$

Note that the asterisk denotes complex conjugation. Consider a simple implementation of the matching network shown in Fig. 3.3(b) might consist of an inductance L as the series element ($Z_S = \omega L$) and a capacitance C as the parallel element ($Z_P = 1/\omega C$). In this case, the complex-valued Equation (3.7) may be solved for the parameters L and C. For example, for a purely resistive load impedance of Z_L = 12.9 kΩ at an operating frequency of ten gigahertz, we find L = 12.8 nH and C = 19.8 aF. Historically, graphical approaches based on the Smith chart have provided a practical approach to determining the necessary circuit elements for an impedance matching network [3]. More recently, commercial software packages have enabled modeling and design of matching circuits by automating the determination of the circuit elements as well as the optimization of the frequency response. In addition, the advent of automated tuners opens the possibility for real-time, adaptive matching networks.

While the implementation of impedance matching networks remains a workhorse technique for microwave and RF circuit design, traditional impedance matching networks may have limited value for broadband measurements in RF nanoelectronic environments for several reasons. First, while matching networks function effectively only over a limited bandwidth, the targeted characterization of RF nanoelectronic devices and their constituent materials often spans tens of gigahertz. Second, the introduction of the matching network introduces additional circuit elements to the measurement platform, further complicating the de-embedding of the intrinsic response of the nanostructure under test. Keep in mind that de-embedding of the broadband nanostructure properties is at times the sole objective of the measurements, particularly in a research and development environment. By contrast, the purpose of a matching network is to maximize the amount of power transferred from the source to the DUT. Finally, where production of novel nanomaterials is not yet uniform or optimized, variations in material components may necessitate tuning or customizing the matching network for each prototype DUT.

3.4 Reflectometer methods for one-port devices

3.4.1 Implementation with a power splitter

Interferometric techniques provide an effective approach to extreme impedance measurements in the microwave regime. One interferometric approach is to integrate the extreme-impedance DUT into a reflectometer [4, 5]. This is achieved by use of a multiport device, such as a power splitter or a hybrid coupler, with one output port of the device terminated by the high impedance DUT and another output port terminated by a high impedance reference device (or series of reference devices). In this configuration, the reflection coefficient of the entire reflectometer will be proportional to a simple algebraic combination of the reflection coefficients of the two high impedance structures. With a proper choice of the reference devices, the reflection coefficient of the entire reflectometer will be close to zero, and thus will present a measurand that is suitable for commercial, 50 Ω RF and microwave test equipment.

Consider the case of a one-port reflectometer based on a three-port power splitter shown in Fig. 3.4. The reference device and the high impedance DUT terminate port 2 and port 3 of the splitter, respectively. The reference device has impedance Z_{ref} and reflection coefficient Γ_{ref} while the DUT has impedance Z_L and reflection coefficient Γ_L. The reflection coefficient of the entire reflectometer structure Γ_m is measured by connecting port 1 to a vector network analyzer (VNA).

Figure 3.4. **Schematic of a one-port reflectometer based on a power splitter**. The reflectometer consists of a power splitter with a reference device (impedance Z_{ref}) and a device under test (impedance Z_L) terminating ports 2 and 3, respectively. The reflection coefficient of the reflectometer, $\Gamma_m = b_1/a_1$, is measured by connecting port 1 of the splitter to

one port of a vector network analyzer. © 2008 IEEE. Adapted, with permission from A. Lewandowski, D. LeGolvan, T. M. Wallis, A. Imtiaz, and P. Kabos, *2008 72nd ARFTG Microwave Measurement Symposium*, (2008) pp. 45-49.

If the splitter is an ideal, broadband, two-resistor power splitter, the three port scattering parameter matrix of will be given by

$$S^{splitter} = \begin{bmatrix} 0 & 1/2 & 1/2 \\ 1/2 & 1/4 & 1/4 \\ 1/2 & 1/4 & 1/4 \end{bmatrix} . \quad (3.8)$$

It follows that Γ_m is given by

$$\Gamma_m = \frac{\frac{1}{4}(\Gamma_{ref}+\Gamma_L)}{1-\frac{1}{4}(\Gamma_{ref}+\Gamma_L)} . \quad (3.9)$$

Note that for the case where $\Gamma_{ref} = - \Gamma_L$, Equation (3.9) simplifies to $\Gamma_m = 0$. In other words, if the reference device has equal magnitude and opposite phase shift to the high impedance device, the reflectometer will present a matched load to the vector network analyzer. By introducing the reflectometer with an appropriately chosen reference device, we have changed the measurand from Γ_L to Γ_m and effectively moved nearer to the center of the Smith chart. Γ_L can be determined from the measurement of Γ_m by

$$\Gamma_L = \frac{4\Gamma_m-(\Gamma_m+1)\Gamma_{ref}}{\Gamma_m+1} . \quad (3.10)$$

There are several important, underlying assumptions to note about this method. First, the reflection coefficient of the reference device, Γ_{ref}, must be known either through accurate modeling or preferably, measurement. Calibration standards such as open circuits, short circuits, and offset short circuits, are suitable reference devices, as they are often readily available and frequently measured in a calibration laboratory. Second, we assume that the incorporation of the extreme impedance DUT into the reflectometer does not alter Z_{ref} or Z_L. Third, we have assumed that the power splitter is ideal in Equations (3.8), (3.9), and (3.10). The approach can be improved by measurement of the scattering parameters of the power splitter, which can be used in place of the ideal scattering parameters in Equation (3.8) in the subsequent analysis.

3.4.2 Implementation with a hybrid coupler

An alternative implementation of a reflectometer for measuring a one-port device is shown in Fig. 3.5. This implementation incorporates a 180-degree, 3 dB hybrid coupler in place of a power splitter [5], [6]. Note that other passive, four-port elements, such as a 90-degree, 3 dB hybrid coupler, may be used in place of the 180-degree, 3 dB hybrid coupler, albeit with

corresponding minor changes to the analysis below. The reference device and the high impedance DUT terminate port 3 and port 4 of the splitter, respectively. Port 1 of a VNA serves as the microwave signal source and is connected to port 1 of the hybrid coupler. The output at port 2 of the coupler is connected to an amplifier of gain G and then to port 2 of the VNA. Assuming that the hybrid coupler is ideal, the four-port scattering parameter matrix for the 180-degree hybrid coupler is given by

$$S^{hybrid} = \begin{bmatrix} 0 & 1/\sqrt{2} & 1/\sqrt{2} & 0 \\ 1/\sqrt{2} & 0 & 0 & -1/\sqrt{2} \\ 1/\sqrt{2} & 0 & 0 & 1/\sqrt{2} \\ 0 & -1/\sqrt{2} & 1/\sqrt{2} & 0 \end{bmatrix} \quad . \tag{3.11}$$

It follows that the transmitted scattering parameter S_{21} measured by the VNA in Fig. 3.5 is

$$S_{21} = \frac{G}{2}\left(\Gamma_L - \Gamma_{ref}\right) \quad . \tag{3.12}$$

Here, as Γ_{ref} approaches Γ_L, the destructive interference within the reflectometer will be maximized and S_{21} will approach zero. The reflection coefficient of the device can be determined algebraically:

$$\Gamma_L = \frac{2S_{21}}{G} + \Gamma_{ref} \tag{3.13}$$

Figure 3.5. **Schematic of a one-port reflectometer based on a hybrid coupler**. The measurement setup consists of a 180º 3 dB hybrid coupler with a reference device (impedance Z_{ref}) and a device under test (impedance Z_L) terminating ports 3 and 4 of the coupler, respectively. The transmitted scattering parameter $S_{21} = b_2/a_1$, is measured by connecting ports 1 and 2 of the hybrid coupler to ports 1 and 2 of a vector network analyzer. The amplifier has gain G. © 2008 IEEE. Adapted, with permission from M. Randus and K. Hoffmann, *2008 72nd ARFTG Microwave Measurement Symposium*, (2008) pp. 40-44.

Comparing the two reflectometer methods, Equation (3.13) for the hybrid-coupler-based reflectometer provides a simpler form than Equation (3.10) and, in turn, more straightforward analysis. Further, the power-splitter-based reflectometer is based on a one-port reflection measurement while the hybrid-coupler-based reflectometer is based on a two-port transmission measurement. Note that although the hybrid-coupler-based measurement uses two ports of a VNA, the DUT is still a one-port device.

The underlying assumptions of the power-splitter-based reflectometer also apply to the hybrid-coupler-based reflectometer. It is also worthwhile to note that both Equation (3.9) and (3.12) involve simple linear combinations of the reflection coefficients of the high

impedance DUT and a high impedance reference device. Physically, this is the result of direct interference of the signal reflected from the DUT with the signal reflected from the reference device. By satisfying the condition Γ_{ref} = - Γ_L, one insures that this interference is destructive. In general, such interferometric approaches to extreme impedance measurements have been found to be effective and the implementation of such approaches is recommended when it can be implemented in the measurement platform. When interferometric approaches are unavailable or impractical, one must resort to analytical comparison of separate measurements, as we will discuss in Chapter 4.

3.5 Statistical measurements

3.5.1 Use of redundant measurements in the reflectometer method

Before discussing an additional interferometric technique with active signal injection, it is useful to discuss some practical considerations, namely the use of statistical measurement techniques. In general, microwave measurement and calibration techniques require the measurement of a minimum number of reference devices in order to determine all of the unknown variables in the measurement process. For example, in order to calibrate a one-port, guided-wave system three known calibration standards must be measured in order to determine the three unknown calibration coefficients. When redundant measurements of reference devices are included in addition to the minimum number of required measurements, an overdetermined system results, which must be solved by one of many possible fitting or optimization techniques. Statistical techniques that make use of redundant measurements have proven to be an effective strategy for improving the statistical uncertainties associated with a given measurement process. Here, two relevant applications of statistical measurements are discussed: application to the reflectometer methods and application to the characterization of a three-port power splitter.

Consider the hybrid-coupler-based reflectometer method described in section 3.4. From Equation (3.13), only one measurement is needed to find the reflection coefficient of the extreme impedance DUT, namely a measurement (S_{21}) made while a reference standard with a known reflection coefficient (Γ_{ref}) is connected to the reflectometer. Suppose instead of a single reference standard, we have a series of N reference standards indexed by k = 1, 2… N. Each reference standard has a known reflection coefficient, Γ^k_{ref}. The reference standards must all be chosen so that Γ^k_{ref} approaches Γ_L, ensuring complete (or nearly complete) destructive interference within the hybrid-coupler-based reflectometer. There will now be N measurements, one with each of the reference standards connected to the coupler, which will be designated S^k_{21}.

There are many strategies for obtaining Γ_L from the redundant measurements. One straightforward approach is to solve the set of de-coupled equations:

$$\Gamma^k{}_L = \frac{2S^k{}_{21}}{G} + \Gamma^k{}_{ref} \tag{3.14}$$

for N different values of $\Gamma^k{}_L$. Then, a value of Γ_L can be obtained from the average of the $\Gamma^k{}_L$ values. If the uncertainties in $\Gamma^k{}_{ref}$ vary significantly from standard to standard, a weighted average of the $\Gamma^k{}_L$ values may be more appropriate. Alternatively, a cost function K may be defined. One possible implementation of K is

$$K = \sum_{k=0}^{N} \left| S^k{}_{21} - \frac{G}{2}\left(\Gamma_L - \Gamma^k{}_{ref}\right) \right| \quad . \tag{3.15}$$

An optimization algorithm may then be used to find a value of Γ_L that minimizes K. A variety of automated optimization approaches exist, many of which can be easily implemented by use of commercial software. Once again, weighting coefficients may be added to the cost function in proportion to the uncertainties in the values of $\Gamma^k{}_{ref}$.

3.5.2 Use of redundant measurements to characterize a power splitter

Another relevant application of statistical measurements is the characterization of a three-port power splitter. This approach is presented here as an additional example of a statistical measurement approach and as a method to improve the reflectometer method. Recall that the accuracy of the power-splitter-based reflectometer method may be improved by using the measured scattering parameters of the power splitter in place of Equation (3.8). Because of the wide availability of conventional two-port VNAs, several approaches have been developed that use a two-port VNA to characterize a three-port device [7],[8]. The technique in reference [7] is extendable to a statistical measurement technique that makes use of redundant measurements [9].

In order to perform the measurement, the two ports of a calibrated VNA are connected to the output terminals of the power splitter (ports 2 and 3), as shown in Fig. 3.6. Note that an adapter with known scattering parameters may be required in order to provide compatibility with and insertable two-port calibration. Known one-port reference standards $\Gamma^k{}_{ref}$ are then connected to the input port of the power splitter (port 1). For each standard, a set of four scattering parameters $S^M{}_{ij}$ are measured (i = 2, 3 and j = 2, 3). The measured $S^M{}_{ij}$ are related to the scattering parameters of the power splitter, S_{ij}, by:

$$S^M{}_{ij} = S_{ij} + \frac{S_{1j} S_{i1} \Gamma^k{}_{ref}}{1 - S_{11} \Gamma^k{}_{ref}} \quad . \tag{3.16}$$

This system of equations has eight unknowns: S_{11}, S_{22}, S_{33}, S_{23}, S_{32}, $S_{13}S_{31}$, $S_{12}S_{21}$, and $S_{12}S_{31}$ (Note that $S_{13}S_{21}$ can be found from the other unknowns). Since there are four equations for each set of measurements made with a given one-port reference standard, the system will be overdetermined if more than two reference standards are used.

Figure 3.6. **Schematic of power splitter measurement**. The output terminals of the power splitter, ports 2 and 3, are connected to a calibrated vector network analyzer. A

series of reference standards are connected to the input port of the splitter, port 1, during measurement. An adapter is inserted to provide compatibility with and insertable two-port calibration. © 2008 IEEE. Adapted, with permission from T. M. Wallis and A. Lewandowski, *2008 72nd ARFTG Microwave Measurement Symposium*, (2008) pp. 50-53.

One approach to solving this system of overdetermined equations begins with multiplying Equation (3.16) by a factor of $1 - S_{11}\,\Gamma^{k}_{ref}$ in order to linearize the equations. The system of linear equations may then be solved by the method of least squares or another form of regression analysis. In turn, these solutions to the linearized problem may serve as initial guesses, or "seeds," for more sophisticated optimization routines.

3.6 Interferometer with active signal injection

So far, we have discussed reflectometers based on passive components, in which the signal reflected from the extreme impedance DUT interfered destructively with the signal reflected from a known reference impedance. Alternatively, an interferometer can be implemented with an actively injected signal in place of the signal reflected from a known impedance [10]. This all-electronic approach eliminates the requirement for a mechanical reference impedance (or set of mechanical reference impedances).

A schematic of the interferometer with active signal injection is shown in Fig. 3.7. A comparison of this measurement platform with the coupler-based reflectometer shown in Fig. 3.5 reveals that both techniques use a hybrid coupler to generate interference between signals and a network analyzer to measure scattering parameters. The VNA reference channel (sometimes referred to as the "R" channel) provides the input signal for a power splitter. An amplified signal from port 2 of the power splitter provides the local oscillator (LO) drive signal for the I/Q mixer. Two DC voltages, $V_{DC,I}$ and $V_{DC,Q}$, are used to adjust the signal phase and amplitude of the output of the I/Q mixer, which is subsequently injected into port 3 of the hybrid coupler. For an ideal coupler, the complex amplitude of the injected signal, b_{inj}, is given by:

$$b_M = \frac{1}{2}(b - b_{inj}) \tag{3.17}$$

where b is the complex amplitude of the signal reflected from the extreme impedance and b_M is the complex amplitude of the reflected wave measured by the VNA. Since b_{inj} can be tuned by the DC voltages $V_{DC,I}$ and $V_{DC,Q}$, a value of b_{inj} can be selected for which b_M approaches zero and complete (or nearly complete) destructive interference occurs. Thus, the measured value $\Gamma_M = b_M/a_M$ will also approach zero, corresponding to a measurement near the center of the Smith chart. For a non-ideal hybrid coupler, Equation (3.17) must be modified to account for non-ideal coupling and loss [10], but the general conclusion remains: the injected signal may be tuned so the destructive interference occurs between it and the signal reflected from the extreme impedance DUT.

Figure 3.7. **Schematic of an interferometer with active signal injection**. The interferometer comprises a vector network analyzer (VNA), 180º 3 dB hybrid coupler, a power splitter, and an I/Q mixer. The signal is taken from the VNA source (labeled RF) and, after emerging from the power splitter, fed back to the VNA reference channel (labeled R). The measurement is made at port 1 of the VNA. A device under test (extreme impedance Z_L) terminates port 2 of the coupler. The injected signal (complex amplitude b_{inj}) is output from the I/Q mixer and interferes destructively with the signal reflected from the device under test (amplitude b). DC bias voltages $V_{DC,I}$ and $V_{DC,Q}$ control the amplitude and phase components of b_{inj}. The reflection coefficient of the reflectometer, $\Gamma_M = b_M/a_M$, is measured. © 2015 IEEE. Adapted, with permission from G. Vlachogiannakis, H. T. Shivamurthy, M. A. Del Pino, and M. Spirito, *2015 IEEE MTT-S International Microwave Symposium (IMS)*, (2015) pp. 1-4.

In order to extract the impedance of the extreme impedance device from the measured Γ_M, the system must be calibrated [11]. The first step is to carry out a one-port calibration at the DUT reference plane, which is shown as a dashed black line in Fig. 3.7. This one-port calibration is carried out with the injection signal turned off. A one-port calibration can be carried out by use of three standards, such as a short, an open and a matched load, for example. As described in Chapter 2, the one-port calibration determines three error terms: the directivity (e_{00}), the source match (e_{11}), and the reflection tracking ($e_{10}\,e_{01}$). Once these error terms are known from the calibration, the reflection coefficient at the reference plane Γ can be determined:

$$\Gamma = \frac{\Gamma_M - e_{00}}{e_{10}e_{01} + e_{11}(\Gamma_M - e_{00})} \quad . \tag{3.18}$$

The second step is to optimize the amplitude and phase of the injected signal. The objective is to tune the injected signal such that the calibrated reflection coefficient of a reference extreme impedance device in the presence of the injected signal, Γ_{ref}, is close to the calibrated reflection coefficient of a matched load in the absence of the injected signal, $\Gamma_{matched}$. Keep in mind that Γ_{ref} and $\Gamma_{matched}$ are both complex quantities. In order to obtain $\Gamma_{matched}$, a matched load is connected at the reference plane and Γ_M is measured with the injection signal turned off. $\Gamma_{matched}$ is then found via Equation (3.18). Subsequently, Γ_{ref} is obtained in a similar fashion, but now with a known extreme impedance connected at the reference plane and the injection signal turned on. The amplitude and phase of the injection signal is then tuned by adjusting $V_{DC,I}$ and $V_{DC,Q}$ until Γ_{ref} is nominally close to $\Gamma_{matched}$.

With the one-port calibration complete and the injection signal optimized, the extreme impedance DUT can now be measured. The extreme impedance DUT is connected at the reference plane and Γ_M is measured with the injection signal turned on and optimized. The calibrated reflection coefficient of the DUT Γ is once again found via Equation (3.18). Since

the injection signal was optimized with the reference impedance Z_{ref} connected at the reference plane, the extreme impedance, the DUT impedance Z_L can be found via [11]:

$$Z_L = Z_{ref}\left(\frac{1-|\Gamma|}{1+|\Gamma|}\right) \quad . \tag{3.19}$$

As in the case of the reflectometer, the reference impedance Z_{ref} must once again be known, either through modeling or measurement. Once again, calibration standards such as open circuits, short circuits, and offset short circuits, may serve as suitable reference devices. The design and fabrication of practical extreme impedance verification devices and standards is an area of ongoing investigation. For example, devices that integrate waveguides operating below cutoff with high-resistance shunts have been proposed as extremely high impedance standards [12].

References

[1] C. Rutherglen and P. Burke, "Nanoelectromagnetics: Circuit and Electromagnetic Properties of Carbon Nanotubes" *Small*, **5** (2009) pp. 884-906.

[2] K. v. Klitzing, G. Dorda, and M. Pepper, "New Method for High-Accuracy Determination of the Fine-Structure Constant Based on Quantized Hall Resistance" *Physical Review Letters*, **45** (1980) pp. 494-497.

[3] H. Jasik, *Antenna Engineering Handbook, 1st Ed.* McGraw-Hill: New York (1961). Section 31.7.

[4] A. Lewandowski, D. LeGolvan, T. M. Wallis, A. Imtiaz, and P. Kabos, "Wideband measurement of extreme impedances with a multistate reflectometer," *2008 72nd ARFTG Microwave Measurement Symposium*, (2008) pp. 45-49.

[5] M. Randus and K. Hoffmann, "A Simple Method for Extreme Impedances Measurement – Experimental Testing" *2008 72nd ARFTG Microwave Measurement Symposium*, (2008) p. 40-44.

[6] M. Randus and K. Hoffmann, "A method for direct impedance measurement in microwave and millimeter-wave bands," *IEEE Transactions on Microwave Theory and Techniques*, **59** (2011) pp. 2123-2130.

[7] M. Davidovitz, "Reconstruction of the S-matrix for a 3-port Using Measurements at Only Two Ports," *IEEE Microwave and Guided Wave Letters*, **5** (1995) pp. 349-350.

[8] J. C. Tippet and R. A. Speciale, "A Rigorous Technique for Measuring the Scattering Matrix of a Multiport Device with a 2-Port Network Analyzer," *IEEE Transactions on Microwave Theory and Techniques*, **30** (1982) p. 661-666.

[9] T. M. Wallis and A. Lewandowski, “Statistical Measurement Techniques for Equivalent Source Mismatch of 1.85 mm Power Splitter,” *2008 72nd ARFTG Microwave Measurement Symposium*, (2008) pp. 50-53

[10] G. Vlachogiannakis, H. T. Shivamurthy, M. A. Del Pino, and M. Spirito, “An I/Q-Mixer Steering Interferometric Technique for High-Sensitivity Measurement of Extreme Impedances,” *2015 IEEE MTT-S International Microwave Symposium (IMS)*, (2015) pp. 1-4.

[11] F. Mubarak, R. Romano, and M. Spirito, “Evaluation and Modeling of Measurement Resolution of a Vector Network Analyzer for Extreme Impedance Measurements,” *2015 86th ARFTG Microwave Measurement Symposium*, (2015) pp. 1-4.

[12] M. Haase and K. Hoffman, “Calibration/Verification Standards for Measurement of Extremely High Impedances,” *2015 86th ARFTG Microwave Measurement Symposium*, (2015) pp. 1-4.

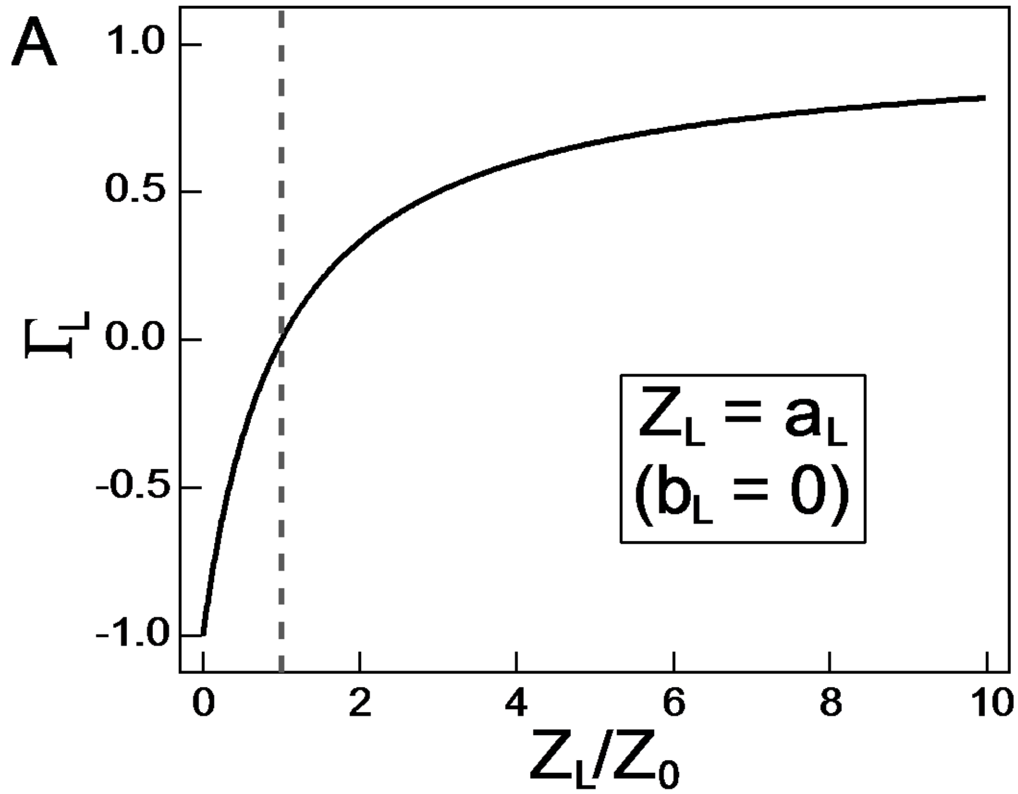

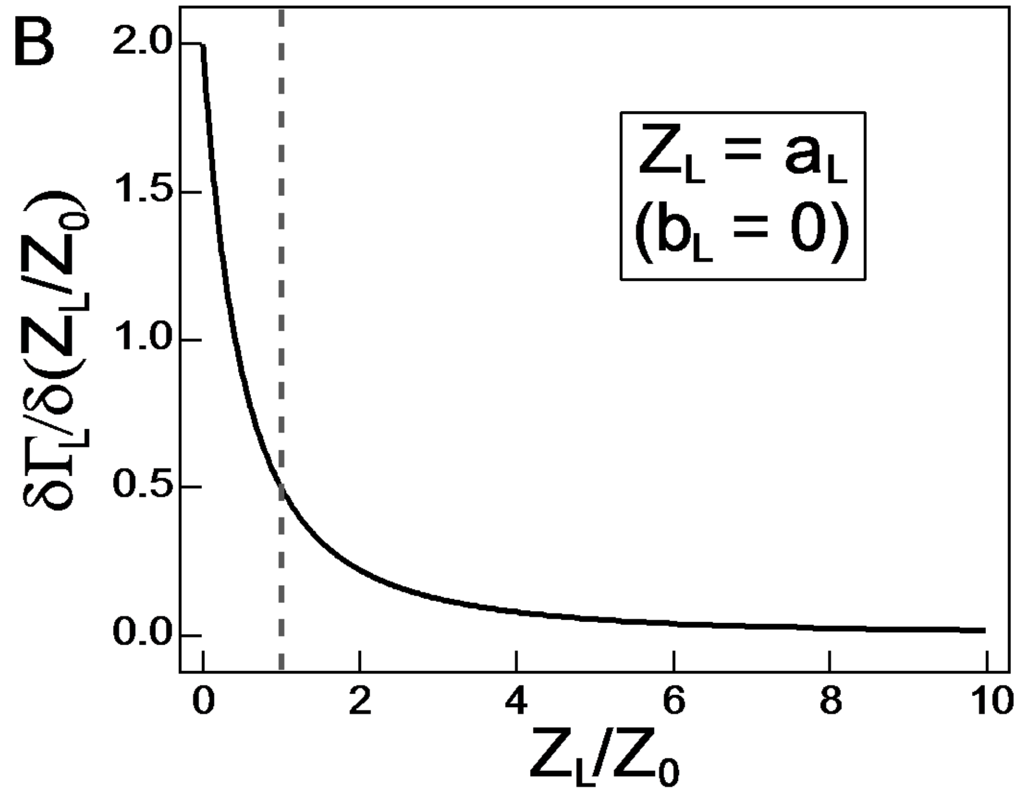

FIGURE 3-1.

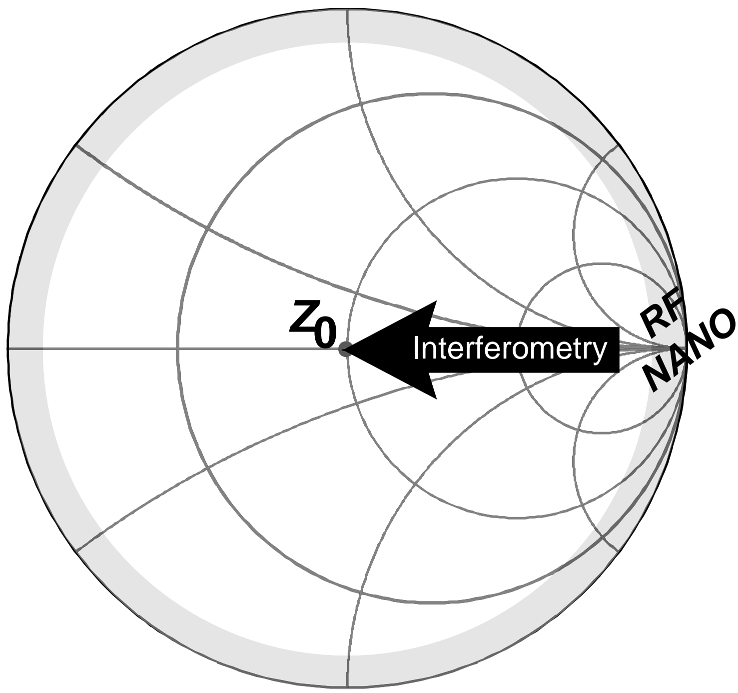

FIGURE 3-2.

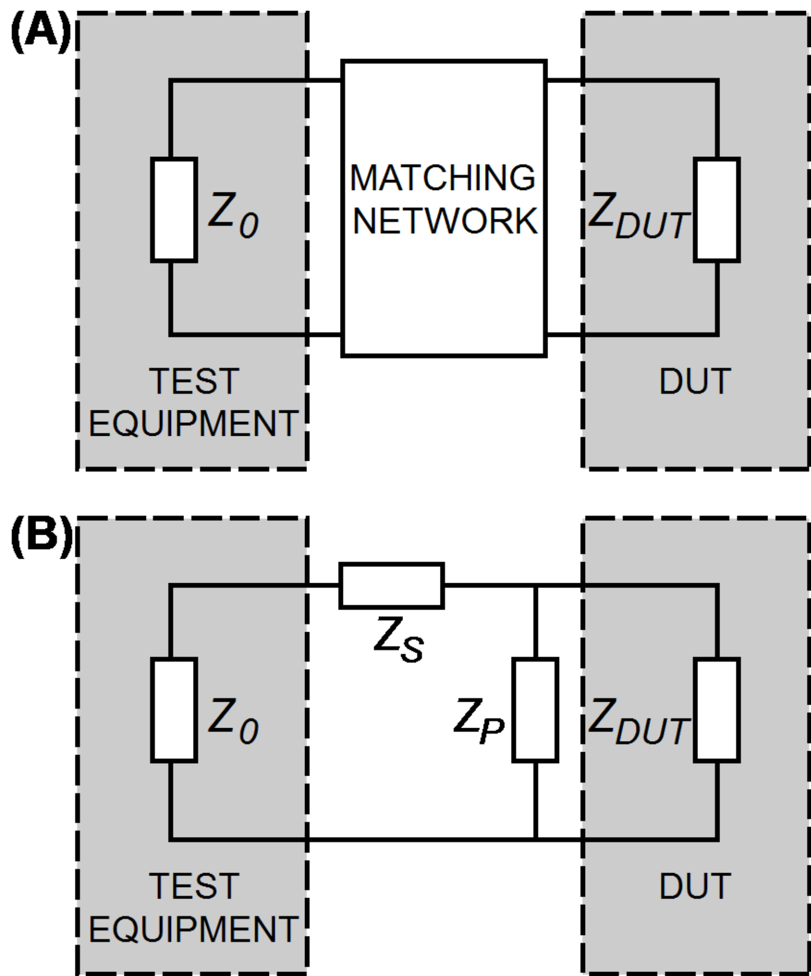

FIGURE 3-3.

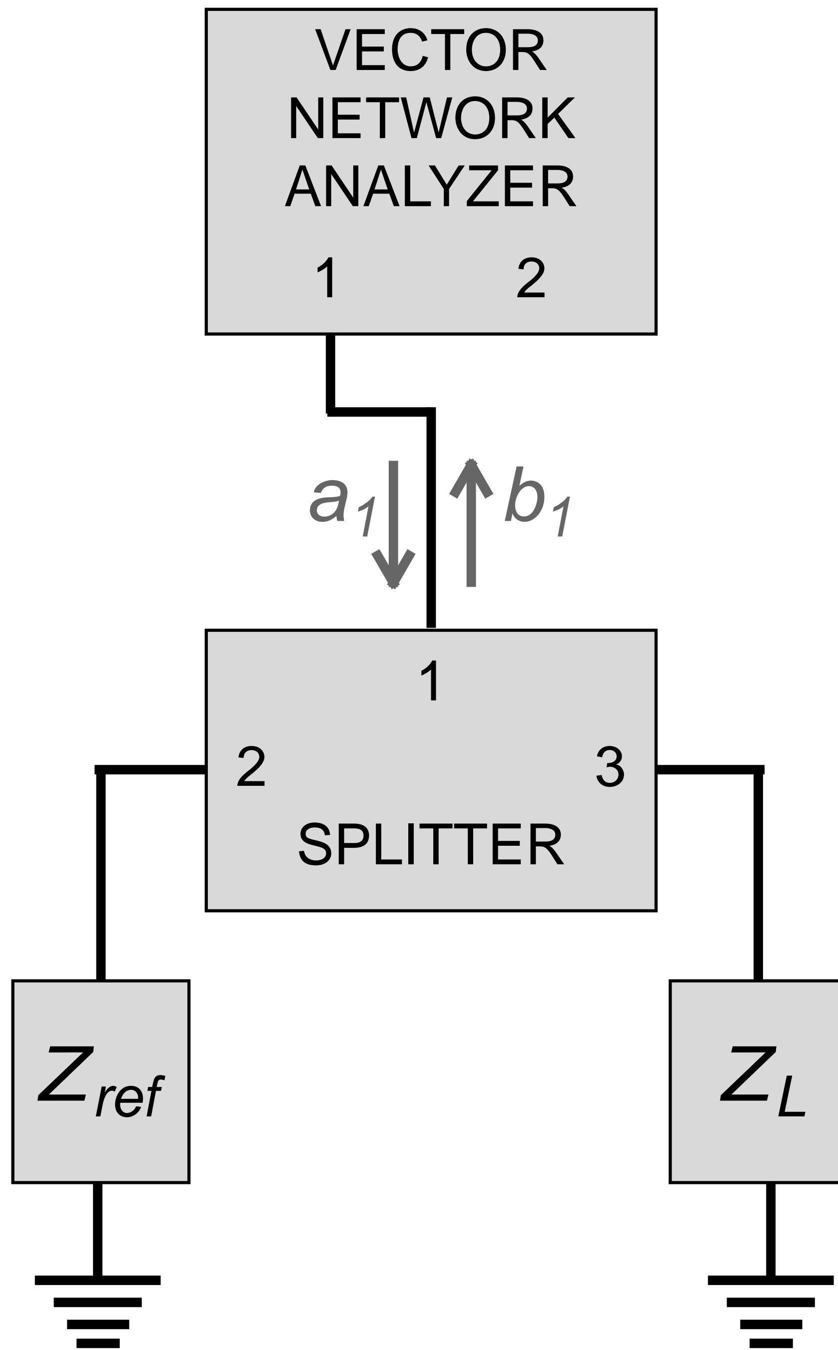

FIGURE 3-4.

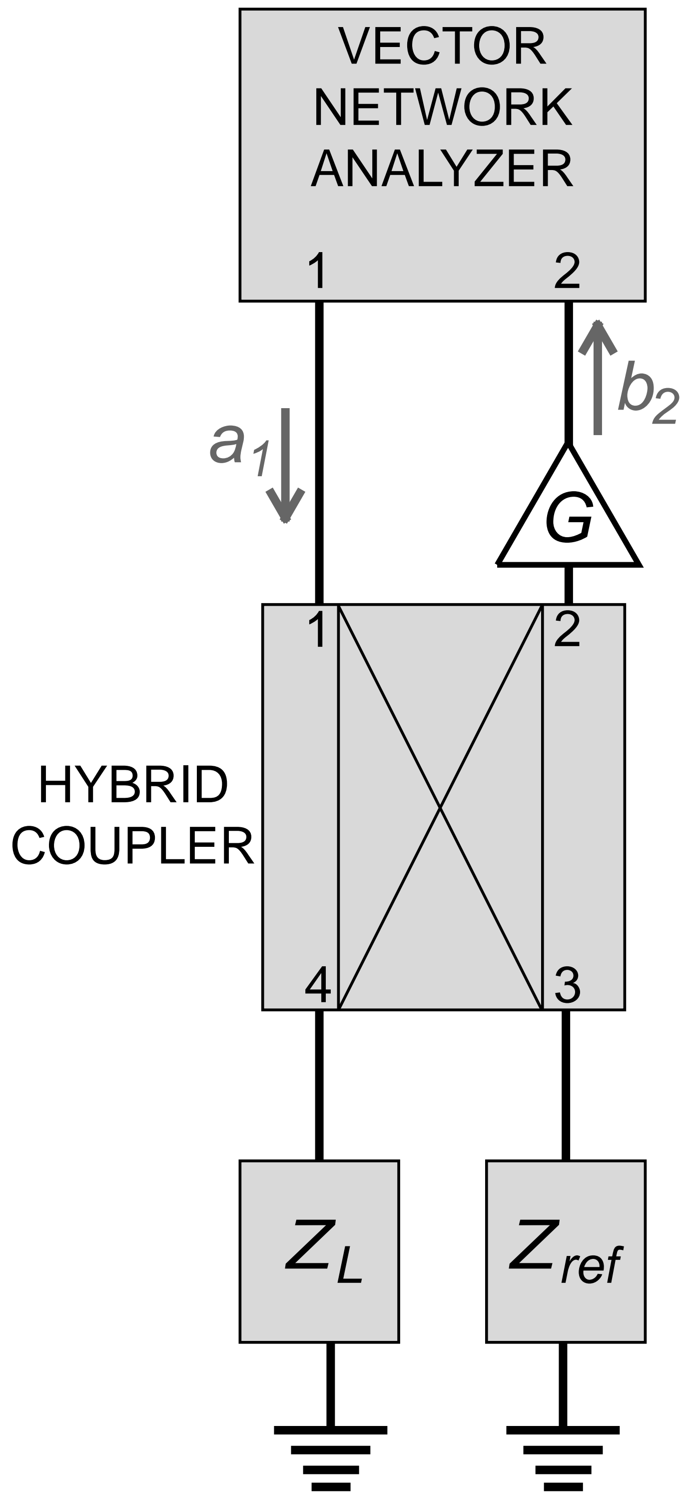

FIGURE 3-5.

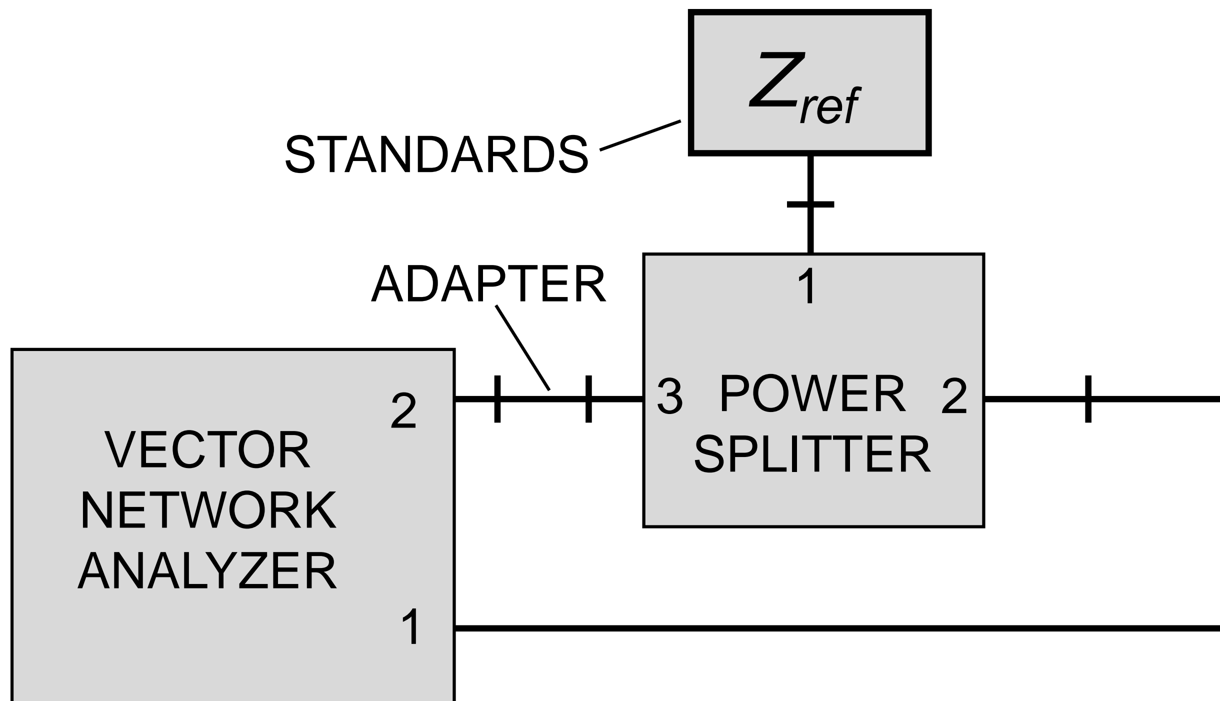

FIGURE 3-6.

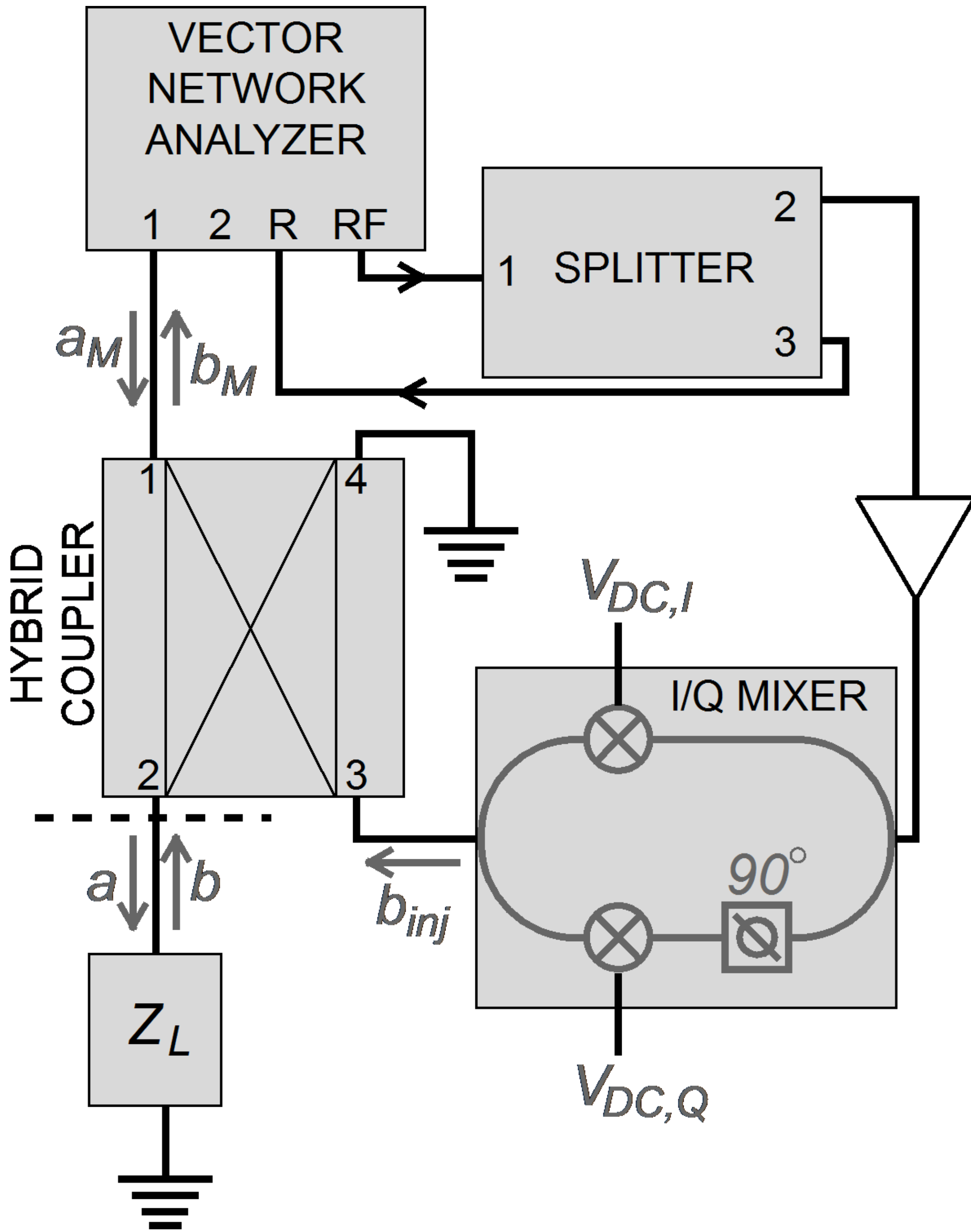

FIGURE 3-7.